Article:

Peng, Z. orcid.org/0000-0003-3918-4479, Smith, C. and Stovin, V. (2019) Internal fluctuations in green roof substrate moisture content during storm events: Monitored data and model simulations. Journal of Hydrology, 573. pp. 872-884. ISSN 0022-1694

https://doi.org/10.1016/j.jhydrol.2019.04.008

Internal fluctuations in green roof substrate moisture content during storm events: Monitored data and model simulations

Zhangjie Peng*, Colin Smith and Virginia Stovin

Department of Civil and Structural Engineering, The University of Sheffield, Mappin Street, Sheffield S1 3JD, United Kingdom.

*Corresponding author

Email addresses: zpeng3@sheffield.ac.uk (Z. Peng), c.c.smith@sheffield.ac.uk (C. Smith). v.stovin@sheffield.ac.uk (V. Stovin).

Keywords: Green roof; Substrate; Detention modelling; Moisture content; Soil water release curve (SWRC); Hydraulic conductivity function (HCF).

Abstract

Understanding how the moisture content in a green roof substrate varies during a storm event is essential for accurately modelling runoff detention. In this paper, a green roof test bed installed with moisture probes at three depths was used to understand how moisture content varies during storms. Detailed studies were conducted on five selected storm events. Physical characterisation tests and field-data based calibrations were performed to acquire the model parameters. Two alternative detention models, based on Reservoir Routing and Richard's Equation, were validated against the measured green roof runoff and temporary moisture storage data. Once the moisture content exceeds local field capacity, its response at different depths occurs simultaneously during storms, although the recorded data indicate

a vertical gradient in the absolute values of local field capacity. Both Reservoir Routing and Richard’s Equation can provide reasonable estimations of the runoff and the vertical moisture content profiles, although Richard’s Equation exhibited stronger vertical water content gradients than were observed in practise. The vertical water content profile is not sensitive to the soil water release curve, although the hydraulic conductivity function influences both the vertical water content profile and runoff rate. The modelled results are highly sensitive to the bottom boundary condition, with a constant suction head boundary condition providing a more suitable option than a free drainage boundary condition or a seepage boundary condition.

1 Introduction

Green roofs can potentially contribute to urban stormwater management through two processes, the retention of rainfall and the detention of runoff. Green roof hydrological performance is a function of a combination of physical processes, and these processes are influenced by the substrate's physical properties. For example, retention performance is strongly influenced by the water release characteristics, which in turn determine wilting point and maximum water holding capacity (De-Ville et al., 2017; Fassman and Simcock, 2012; Liu and Fassman-Beck, 2016). It is widely understood that moisture lost via evapotranspiration prior to a storm event provides retention capacity within the substrate. It has also been demonstrated that in a shallow green roof system, losses due to evapotranspiration reduce when there is restricted moisture available (Poë et al., 2015; Voyde et al., 2010). This conceptual understanding of retention processes is widely adopted in green roof hydrological models.

However, green roof detention processes are less well understood, and therefore less consistently represented in green roof hydrological models. It is widely accepted that detention is of great interest to stormwater engineers and planners. Detention processe determine the timing and magnitude of peak runoff to the downstream sewer network. The attenuation and lag of peak runoff may mitigate the risk of localised flooding and reduce the frequency of combined sewer overflows (CSOs). Many previous studies on green roof detention have focused on observed performance, using different metrics to characterise detention from monitored rainfall and runoff data. However, detention performance metrics – such as Peak Attenuation – can be influenced by many factors, including rainfall characteristics and antecedent conditions (Stovin et al., 2017). Such metrics do not provide generic modelling capability, in terms of the ability to estimate the temporal runoff profile associated with an unseen rainfall event applied to an unmonitored green roof.

Whilst detention performance metrics are dependent upon external factors such as rainfall inputs, the underlying detention processes are independent of these factors, and depend only on the roof's physical configuration (e.g. its slope, substrate characteristics and drainage layer configuration etc.). Detention performance is dependent upon the substrate's hydraulic conductivity and porosity, as these properties determine the speed of the water flowing through the substrate (De-Ville et al., 2017; Liu and Fassman-beck, 2018; Liu and Fassman-Beck, 2017).

Techniques used to model detention include Reservoir Routing (a 'black-box', empirical approach), a simplified physically-based model in the USEPA's Storm Water Management Model (SWMM) and unsaturated flow models based on the Richard's Equation. All these models have demonstrated acceptable levels of accuracy for modelling runoff detention (Castiglia Feitosa and Wilkinson, 2016; Hilten et al., 2008; Kasmin et al., 2010; Liu and Fassman-Beck, 2017; Palla et al., 2012; Peng and Stovin, 2017; Soulis et al., 2017).

As an example of an empirical approach, Stovin et al. (2015) utilised data from nine differently-configured green roof test beds to identify suitable Reservoir Routing parameters, suggesting that the empirically-derived parameter values reflected differences in the basic configuration (vegetation and substrate components) of individual test beds. However, no direct links between roof components and detention model parameters were established.

The physically-based model, Richard's Equation, potentially has more generic application, as, unlike the Reservoir Routing model, the parameters depend on measurable physical properties rather than on previously-monitored data. However, Richard's Equation models depend upon certain models and assumptions about unsaturated flow in soils, that may not be fully applicable within non-uniform, coarse-grained, heterogeneous green roof substrates.

Green roof detention models have typically been validated based on the runoff exiting the substrate or the whole green roof system (Kasmin et al., 2010; Liu and Fassman-Beck, 2017; Palla et al., 2009, 2012; Vesuviano et al., 2014; Yio et al., 2013). For example, Liu and Fassman-Beck (2017) validated the Richard's Equation using measured runoff below a column of green roof substrate. Hakimdavar et al.(2014) regenerated the runoff profiles of three green roofs in response to various storms using Richard's Equation. However, in both studies, validation of the internal vertical water content profile was not reported. Vertical water content profiles reflect the volume of water temporarily stored in the substrate. As the stored water leaves the green roof system as runoff, correctly modelling the timing and the volume of temporary storage is critical to detention modelling. As a physically based model, it is expected that Richard's Equation should be capable of modelling not only the runoff from the bottom, but also the dynamic temporary storage within the substrate. However, only a limited number of studies have investigated green roof detention from the perspective of vertical unsaturated flows within the substrate. Palla et al. (2009) validated the Richard's Equation (2D form) with modelled runoff from a full-scale green roof. The modelled vertical water content profile was compared with measured data at only a few points in time, and the comparisons suggested that the Richard's Equation tends to underestimate the water content in the substrate. It is evident that continuous time-series data characterising moisture content variations within the substrate would provide a valuable addition to the literature on green roof detention.

In a full-scale green roof system, detention effects will also include delays due to the runoff passing through the drainage layer (Stovin et al., 2015). The two-stage green roof detention model proposed by Vesuviano et al. (2014) took account of the effect of the drainage layer, with two separate Reservoir Routing models being used to represent detention due to the substrate and drainage layer respectively. A similar approach was adopted by Palla et al. (2012), who applied a linear Reservoir Routing model to represent the lateral flow to the collection barrel. Figure 1 provides a schematic illustration of the conceptual hydrological model outlined above, indicating the two options for representing substrate detention: Reservoir Routing and Richard's Equation.

Fig. 1. Conceptual green roof hydrological model: left – vertical profile through a typical green roof system indicating the layers associated with retention and detention processes; right – components of a two-stage detention model, indicating the two alternative options for representing substrate detention considered in the present paper.

The aim of this study is to understand the moisture content dynamics within a green roof substrate during storm events and to compare field observations with model simulations made using both a Reservoir Routing model and the Richard's Equation. The aim is achieved via the following objectives:

- Experimentally characterise the relevant green roof substrate physical properties;
- Utilise the moisture content data collected from a green roof test bed to explore changes in substrate moisture content during storm events;

- Validate the Reservoir Routing model and the Richard's Equation based on observed runoff, observed temporarily stored moisture and observed vertical moisture content profiles (Richard's Equation only);
- Assess the sensitivity of predictions made with the Richard's Equation to the water release curve, hydraulic conductivity function and bottom boundary condition.

2 Methods

2.1 Experimental set up

2.1.1 The test beds

The test site, located on a fifth-floor terrace of the Sir Robert Hadfield building (53.3816, -1.4773), the University of Sheffield, UK, consists of nine green roof test beds (TBs) which vary systematically in substrate composition and vegetation treatment. The experiment was established in 2009 and the rainfall-runoff data was collected from April 2010. Each test bed is 3 m long × 1 m wide with 1.5° slope. The test beds consist of an impermeable hard plastic tray base, a drainage layer (Zinco Floradrain FD 25-E), a filter sheet (Zinco Systemfilter SF) and one of nine substrate (80 mm deep) and vegetation combinations. On-site climate data, including temperature, solar radiation, wind speed and relative humidity, were recorded by a Campbell Scientific weather station at 1-hour intervals. 0.2 mm resolution AGR-100 tipping bucket rain gauges manufactured by Environmental Measures Ltd. were used to record the on-site rainfall. A collection tank equipped with Druck Inc. PDCR 1830 pressure transducer under each test bed was used for runoff measurement at 1 min intervals. The pressure transducers were calibrated against volumes on site. A full description of the test beds can be found in Berretta et al. (2014); De-Ville et al. (2018); and Stovin et al. (2015).

Test bed 1 (TB1) is a sedum vegetated green roof with heather and lavender substrate (HLS), and TB7 is an unvegetated bed with HLS substrate. Both test beds were equipped with moisture content sensors. The other seven TBs are not relevant to the present study.

Substrate moisture content data was collected from March 2011. Three water content reflectometers (Campbell Scientific CS616), inserted at 20 mm (Top), 40 mm (Mid) and 60 mm (Bottom) below the surface of the green roof, provide continuous water content measurement at 5-minute intervals. The rods of the mid and top probes were installed 90° and 180° respectively from the lower one in order to avoid interference of the measurement reading taken by the probes. A diagram showing the location of the moisture probes can be found in Berretta et al. (2014). The water content reflectometers were calibrated at 20°C in a laboratory environment from 0.05 to 0.40 v/v and an appropriate temperature correction was applied. The moisture content in the substrate could exceed 0.4 v/v during storms. However, it is not straightforward to calibrate the moisture probes above 0.4 v/v with our substrates due to the rapid drainage of water that occurs once the moisture content exceeds field capacity.

2.1.2 Substrate characteristics

The Forschungsgesellschaft Landschaftsentwicklung Landschaftsbau (FLL) (FLL, 2008) provides the standard guidance for determining green roof substrate physical properties. The FLL outlines a range of laboratory test methods, apparatus, and standard target values for substrates to achieve design functions. Properties determined include particle size distribution, maximum water holding capacity and water permeability (saturated hydraulic conductivity). Whilst the saturated hydraulic conductivity should provide some indication of detention behaviour, some questions have been raised about the usefulness of the FLL permeability test. Researchers have reported considerable variation in repeat and replicate determinations of permeability (Fassman and Simcock, 2012; Stovin et al., 2015).

Utilisation of the Richard's Equation requires more fundamental physical properties derived from soil science, such as the water release curve and the unsaturated hydraulic conductivity function (Berretta et al., 2014; Liu and Fassman-beck, 2018; Liu and Fassman-Beck, 2017). The water release curve is a reflection of the substrate's ability to store water (retention and temporary storage capacity) and the unsaturated hydraulic conductivity is an indicator of the substrate's water conducting ability (detention performance). As green roof substrates are not expected to ever reach saturation, the unsaturated hydraulic conductivity characteristics are more relevant to green roof hydrological modelling than the saturated hydraulic conductivity (Fassman and Simcock, 2012; Liu and Fassman-Beck, 2018).

HLS is a brick-based substrate comprising crushed bricks, pumice and organic matter including compost with fibre and clay materials. Basic physical properties (bulk density, porosity, maximum water holding capacity, permeability and particle size distribution) were determined for the HLS substrate following the FLL guidance (FLL, 2008). To minimise the uncertainties associated with subsampling, each test was conducted with three replications.

The soil water release curve (SWRC) for the HLS substrate was determined by the pressure plate extraction and hanging column methods. The hanging column method was used to determine the points on the SWRC at suction heads of 6 cm to 100 cm and the pressure extractor method was used for high suction heads from 330 cm to 15000 cm. The data points measured by the pressure extractor method were previously reported by Berretta et al. (2014) whilst the data points for low suction heads, using the hanging column method, were newly determined and added to the dataset for model fitting. At high suction heads, the SWRC reflects the difficulty of water extraction from the substrate during dry weather periods; the water release curve at low suction heads is more relevant to detention processes during storm events.

2.2 Data analysis

The monitored moisture content data spans the period from March 2011 to February 2016. It was found that 92 out of the 444 identified events had complete and reliable rainfall and runoff records for TB1 and TB7; these events are referred to as 'valid' events. The rainfall-runoff data collected from 2010 was used to calibrate Reservoir Routing model parameters, and five representative storm events were selected for model validation. Table 2 lists the characteristics of the five selected storm events, the performance of TB1 in response to the storms and the observed initial water content. The monitored rainfall-runoff data for TB7 was used to derive Reservoir Routing model parameters for the drainage layer and the rainfall-runoff and moisture content data for TB1 was used to validate the substrate models and investigate the moisture content behaviour during storms.

Table 2. Hydrological characteristics of the five selected storm events and TB1 hydrological performance

2.3 Detention modelling

Two approaches are commonly taken to model the detention effect in the substrate: a lumped (black box) approach based on Reservoir Routing; or a physically-based finite element approach based on unsaturated flow hydraulics and the Richard's Equation (e.g. as implemented in the widely-used HYDRUS-1D model). During a storm event the substrate moisture content temporarily rises above field capacity, leading to the generation of runoff.

In this study, to account for the detention effects in the drainage layer, a two-stage green roof detention model, as proposed by Vesuviano et al. (2014) and Palla et al. (2012), was used. Two alternative options for modelling the substrate detention were considered here: a Reservoir Routing model and the Richards's Equation. A second Reservoir Routing equation was used to represent the detention effect in the drainage layer (Fig. 1). The modelled runoff and the temporary storage in the substrates were compared with the monitored data to evaluate the performance of the models. R_t^2 (Young et al., 1980) was used to describe the goodness of fit between modelled and monitored runoff.

2.4 Substrate detention models

2.4.1 The Reservoir Routing model

The lumped Reservoir Routing model is given by the following equations:

$$\boldsymbol{Qout_t = kh_{t-1}^n} \tag{1}$$

$$\boldsymbol{h_t = h_{t-1} + Qin_t \Delta t - Qout_t \Delta t} \tag{2}$$

where $\boldsymbol{Qin}$ is the inflow due to rainfall in mm/min, $\boldsymbol{Qout}$ is the runoff from the green roof substrate in mm/min, $\boldsymbol{h}$ is the stored water, in mm, $\Delta\boldsymbol{t}$ is the discretisation time step and $\boldsymbol{k}$ ($mm^{(1-n)}$ /min) and $\boldsymbol{n}$ (dimensionless) are routing parameters.

2.4.2 The Richard's Equation

The 1-D vertical Richard's Equation is given as follows:

$$\boldsymbol{\frac{\partial \theta}{\partial t} = \frac{\partial}{\partial Z}\left[K(h)\left(\frac{\partial h}{\partial Z} - 1\right)\right]} \tag{3}$$

where $\boldsymbol{\theta}$ is volumetric water content, $\boldsymbol{K(h)}$ is hydraulic conductivity at suction head $\boldsymbol{h}$ and $\boldsymbol{Z}$ is the elevation of the point relative to the reference level. To solve Richard's Equation, functions describing the relationship between volumetric water content and suction head (Soil Water Release Curve, SWRC) and the relationship between unsaturated hydraulic conductivity and volumetric water content or suction head (Hydraulic Conductivity Function, HCF) are needed. For initial investigations, the Durner equation (Durner, 1994) (Eq. 6, 7, and 8) was used for SWRC, and the Durner-Mualem equation (Eq. 9) was used to estimate unsaturated hydraulic conductivity as a function of suction head. Further investigations were conducted using the Van-Genuchten model (van Genuchten, 1980) (Eq. 4) for SWRC and the Van-Genuchten-Mualem equation (Mualem, 1976) (Eq. 5) for HCF. The Durner equation and a new HCF equation (Marshall et al., 1996) (Eq. 10) were also used to investigate the influence of the HCF.

$$S_e = \frac{\theta-\theta_r}{\theta_s-\theta_r} = [1+(\alpha h)^n]^{-m} \tag{4}$$

$$K(S_e) = K_s S_e^{\tau}\left[1-(1-S_e^{1/m})^m\right]^2 \tag{5}$$

$$S_e = \frac{\theta-\theta_r}{\theta_s-\theta_r} = w[1+(\alpha_1 h)^{n_1}]^{-m_1} + (1-w)[1+(\alpha_2 h)^{n_2}]^{-m_2} \tag{6}$$

$$S_{e_1} = [1+(\alpha_1 h)^{n_1}]^{-m_1} \tag{7}$$

$$S_{e_2} = [1+(\alpha_2 h)^{n_2}]^{-m_2} \tag{8}$$

$$K(S_e) = K_s(wS_{e_1}+(1-w)S_{e_2})^{\tau}\frac{\left\{w\alpha_1\left[1-\left(1-S_{e_1}^{1/m_1}\right)^{m_1}\right]+(1-w)\alpha_2\left[1-\left(1-S_{e_2}^{1/m_2}\right)^{m_2}\right]\right\}^2}{(w\alpha_1+(1-w)\alpha_2)^2} \tag{9}$$

$$K(\theta) = a\theta^b \tag{10}$$

where S_e, S_{e1} or S_{e2} is the relative saturation, θ is volumetric water content, θ_r is residual water content, θ_s is saturated water content, h is suction head, a, b, α, n, m, w, α_1, n_1, m_1, α_2, n_2, m_2 are empirical parameters, α is the inverse of air-entry value, n is a pore size distribution index and $\boldsymbol{m = 1 - \frac{1}{n}}$, $\boldsymbol{K_S}$ is saturated hydraulic conductivity, $\boldsymbol{K(S_e)}$ is the unsaturated hydraulic conductivity at $\boldsymbol{S_e}$, $\boldsymbol{K(\theta)}$ is the unsaturated hydraulic conductivity at $\boldsymbol{\theta}$ and the tortuosity parameter, $\boldsymbol{\tau}$ is assumed to be 0.5.

2.5 The drainage layer model

For a green roof with a drainage layer, it is expected that detention will occur as the runoff drains through the drainage layer, and the delay depends on the roof length and drainage layer configuration (Stovin et al., 2015; Vesuviano et al., 2014; Vesuviano and Stovin, 2013). Previous studies have confirmed that different types and dimensions of drainage layers may have different detention characteristics, and a simple nonlinear storage routing model, for which the parameters only depend on the drainage layer physical characteristics, is capable of modelling this effect (Vesuviano et al., 2014; Vesuviano and Stovin, 2013; Palla et al., 2012). In this study, a nonlinear Reservoir Routing equation (Eq. 1 and 2, where $\boldsymbol{Qin}$ is the inflow to the drainage layer from the substrate and $\boldsymbol{Qout}$ is the runoff from the drainage layer) was applied to model the drainage layer detention.

2.6 Model Implementation

As illustrated in Fig. 1, the rainfall-runoff model is characterised by three processes: initial losses (retention); detention due to the substrate; and detention due to the drainage layer. As the focus of the present study is on the second process, substrate detention, it was necessary to eliminate the effects of retention and drainage layer detention from the monitored rainfall and runoff data.

2.6.1 Retention

To model the detention for each selected event, the retention, which was calculated as the difference between the monitored rainfall and runoff depths, was removed from the start of the rainfall profile such that only net rainfall was routed to runoff.

2.6.2 Reservoir Routing parameters for the drainage layer

The drainage layer is consistent between all test beds. Reservoir Routing parameters for the drainage layer were identified by eliminating the effects of substrate detention from monitored runoff responses from TB7. TB7 data is used here for two reasons: firstly, because its substrate is comparable to one that has been assessed in independent laboratory detention tests; and secondly because it is an unvegetated system, so no additional detention effects that might be associated with vegetation or roots are expected.

A substrate specific study (Yio et al., 2013) showed that the parameter $\boldsymbol{k}$ for the substrate Reservoir Routing model ($\boldsymbol{k_g}$) (subscript $\boldsymbol{g}$ refers to growing media) relates to the depth and the permeability of the substrate. The $\boldsymbol{k_g}$ value is transferable between substrates if they have similar components, depth and physical properties. The HLS substrate in TB7 has the same properties as the substrate studied in Yio et al. (2013). Therefore, the TB7 substrate Reservoir Routing coefficients $\boldsymbol{k_g}$ and $\boldsymbol{n_g}$ were assumed to correspond to the values presented there (0.212 $mm^{(1-n)}$/min and 2.0 respectively).

The $\boldsymbol{k_D}$ and $\boldsymbol{n_D}$ values for the drainage layer were then calibrated from the net rainfall and runoff data from TB7 by fixing the substrate parameters to 0.212 $mm^{(1-n)}$/min and 2.0 respectively. Using the TB7 data from the 92 valid storm events, the median calibrated values of $\boldsymbol{k_D}$ and $\boldsymbol{n_D}$ were found to be 0.026 $mm^{(1-n)}$/min and 1.196 respectively). These parameter values were applied to represent the drainage layer detention in subsequent analyses. The reservoir routing models were all run at 5-minute time steps.

2.6.3 Reservoir Routing parameters for the substrates

As TB1 is a vegetated green roof, even though it shares the same substrate with TB7, the presence of vegetation could provide extra detention effects, so the substrate Reservoir Routing parameter ($\boldsymbol{k_g}$) for this test bed needs to be calibrated from monitored rainfall-runoff data. Calibration was conducted with the net rainfall-runoff data from the 92 valid events by fixing $\boldsymbol{k_D}$ to 0.026 mm$^{(1-n)}$/min and $\boldsymbol{n_D}$ to 1.196 (the calibrated values from TB7). $\boldsymbol{n_g}$ was fixed at a value of 2.0 based on the finding of Yio et al. (2013), who demonstrated that model performance was insensitive to changes in its value. The calibrated median value of $\boldsymbol{k_g}$ for TB1 is 0.175 mm$^{(1-n)}$/min (Table 1).

Table 1. Value of parameters used in the Reservoir Routing Model

2.6.4 Richard's Equation

2.6.4.1 SWRC and HCF parameters

To simulate the substrate detention effects using Richard's Equation, the SWRC and HCF parameters are required. Both the Van-Genuchten model (Eq. 4) and the Durner Equation (Eq. 6, 7 and 8) were fitted to the data points on the SWRC measured by the hanging column and pressure plate extractor methods. The fitting and parameter determination were performed using the SWRC Fit software (Seki, 2010). Initial simulations were conducted with the Durner Equation and Durner-Mualem Equation (Eq. 9). The saturated hydraulic conductivity used within the Mualem Equation was determined by the FLL tests ($\boldsymbol{K_s}$ = 25 mm/min, Table 4). For further investigations, the Van-Genuchten-Mualem Equation (Eq. 5) and a new HCF (Eq. 10) were also applied to investigate the influence of SWRC and HCF on the model results.

2.6.4.2 Boundary and initial conditions

For each rainfall event, the upper boundary was set as a Neumann condition in which the surface flux equals the net rainfall input $\boldsymbol{R}$ (Eq. 11); the lower boundary was set to be a constant suction head. The relevant suction head was calculated from the vertically averaged monitored water content two hours after the rainfall stopped. This value is taken to represent field capacity (De-Ville et al., 2018; FLL, 2008). The initial condition was set to be a constant hydraulic head. The moisture content at mid-depth of the substrate was set to the value of field capacity and the suction head of this middle point was calculated from the SWRC. The suction heads for the rest of the vertical profile were calculated according to Eq. 12.

$$\boldsymbol{K(h)\left(\frac{\partial h}{\partial Z}-1\right)=R} \tag{11}$$

where R is the net rainfall (cm/min) and all the symbols are as defined before.

$$\boldsymbol{h_i = h_{i+1} - Z_i + 4} \tag{12}$$

where $\boldsymbol{h_i}$ (cm) is the suction head at point $\boldsymbol{i}$ and $\boldsymbol{Z_i}$ (cm) is the elevation of point i. The upper layer of the substrate was assigned a value of $i = 1$. The reference level of elevation (i.e. $\boldsymbol{Z}$ = 0.0 cm) is at the bottom of the substrate, and the value of 4 in Equation 12 represnts the elevation of the middle depth of the substrate.

The Richard's Equation was solved in MATLAB using the internal PDE solver by discretising the 80 mm of substrate into 101 node points. The Richard's Equation model was run at 5-minute time steps. The drainage layer Reservoir Routing model was adopted to model the lateral flows in the drainage layer and generate the runoff from TB1. The parameters for the drainage layer were the calibrated values as determined before.

3 Results

3.1 Moisture content behaviour during storms

As Table 2 shows, the five selected storms include events in all four seasons. Individual storm events were defined as being separated by at least 6 hours' continuous dry period (Stovin et al., 2012). All events had > 8 mm rainfall and generated at least 5 mm runoff. The 21/Oct/2013 event is the heaviest storm with a return period of greater than one year. No rainfall was retained in the test bed during this storm, which suggests that the test bed was already at field capacity. In contrast, the 26/Aug/2015 event had a relatively long antecedent dry weather period (ADWP) and the return period for this event is less than 1 year. In this storm event, 61% of the rainfall was retained by the green roof test bed.

Fig. 2 presents the rainfall, runoff and moisture content data from TB1 for the five selected rainfall events. Temporary increases in moisture content may be seen to occur in response to rainfall, after which the monitored moisture content returns to a constant value (assumed equal to field capacity). The vertical dashed line indicates the time when the first significant runoff was observed, the dotted line is the time when rainfall stopped, the vertical solid line is two hours after rainfall stopped and the corresponding measured volumetric moisture content is interpreted as the local field capacity (Table 3). Any further reduction below field capacity is expected to be due to evapotranspiration. During the events for which the substrate initial moisture content was below local field capacity (6/Dec/2012 24/May/2014 and 26/Aug/2015), a significant increase in moisture content was witnessed in the substrate at the beginning of the storm prior to the onset of runoff. In the event where the substrate was relatively dry (26/Aug/2015) a wetting front (i.e. a delay in the rise of volumetric water content at the bottom of the substrate compared with the top) was evident. Once the substrate moisture content reached local field capacity, it tended to increase simultaneously with rainfall. The maximum temporary storage in the substrate during the selected storms was generally less than 0.06 v/v, equivalent to 4.8 mm in an 80 mm deep roof. In general, runoff was generated after the substrate reached local field capacity, but runoff was generated before the lower substrate reached its local field capacity in the event on 6/Dec/2012, which may indicate preferential flow.

Table 3 lists the local field capacity determined for each event. The three moisture content probes indicate slightly different moisture content levels at field capacity. Differences in the absolute values are to be expected in coarse-grained heterogeneous green roof substrates that may have consolidated over time. The lowest field capacity was found for the event on 25/Aug/2015 and the highest field capacity was associated with the event on 8/Nov/2014, which is believed to be caused by the seasonal variation of substrate physical characteristics (De-Ville et al., 2018).

Fig. 2. Monitored rainfall, runoff and moisture content profiles for the five selected storm events (vertical dashed line indicates the time significant runoff was firstly observed, dotted line represents the time rainfall stops, the solid vertical line is the time two hours after rainfall stops and the corresponding volumetric water content is assumed to indicate local field capacity).

Table 3. Local field capacity determined for each storm event

3.2 Substrate characteristics

Table 4 lists the results of FLL tests for the HLS green roof substrates. The maximum water holding capacity determined by the FLL tests is close to the average local field capacity (0.385 vs 0.384), which indicates that the FLL tests do provide reasonable estimations of on-site field capacity.

Table 4. HLS Substrate characteristics according to FLL (2008) test methods

Fig. 3(a) presents the measured points and fitted water release curves for the HLS substrate. SWRC A is the fitted Van-Genuchten model and SWRC B is the fitted Durner model. Both models were fitted using the full experimental dataset, determined by the hanging column and pressure plate extractor methods. As fig. 3(a) shows, only minor differences were present between the two models. However, the Durner model has a slightly higher R^2 value (Table 5), which indicates a better fit to the measured data. This may indicate that the green roof substrate is more likely to be a dual porosity system (Liu and Fassman-Beck, 2017). Table 5 lists the calibrated parameters for the Van-Genuchten (SWRC A) and Durner (SWRC B) models. The Fitted Durner parameters (SWRC B) were used in the Richard's Equation to generate the runoff and vertical water content profile, but further investigation was conducted with the Van-Genuchten model in the Discussion section.

Table 5. Fitted parameters for the water release curves for the HLS substrate

Application of the Richards' Equation requires data on the substrate's unsaturated hydraulic conductivity in the form of a Hydraulic Conductivity Function (HCF). Typically, the HCF is derived from the SWRC via the Mualem model. Figure 3(b) shows the Durner-Mualem (SWRC B) and Van-Genuchten-Mualem (SWRC A) derived HCFs for the HLS substrate. However, previous authors have questioned the applicability of these derived HCFs to coarse-grained heterogeneous green roof substrates (e.g. Liu and Fassman-Beck, 2018). Figure 3(b) therefore includes a third HCF, which has been derived from preliminary laboratory tests (based on the ASTM steady state infiltration column test method (ASTM, 2015)) undertaken on the HLS substrate. Given the sparse nature of this preliminary data set, the basic HCF model presented in Equation 10 has been fitted to the data. Substantial differences may be observed between the Mualem-based HCF functions and the new function derived from laboratory measurements. Whilst further work is required to refine the testing procedures and to extend the laboratory data coverage, it is nonetheless interesting to investigate how the alternative HCF would affect the model's prediction of substrate runoff detention. The sensitivity of model predictions to the HCF is therefore considered in the discussion section.

Fig. 3. Water release curves and hydraulic conductivity functions. (a) SWRC A is fitted by the Van-Genuchten model, SWRC B is fitted by the Durner model, both models were fitted using hanging column and pressure plate extractor data; (b) plots of the new HCF and the HCFs derived from the two SWRC in (a) via the Mualem model.

3.3 Model Validation

Fig. 4 compares modelled and monitored runoff from the test bed in response to the five selected storm events. Note that for both substrate detention models the detention due to the drainage layer was modelled using the calibrated Reservoir Routing model described in Section 2.5. With most R_t^2 values higher than 0.6, it is confirmed that both Reservoir Routing and Richard’s Equation can achieve satisfactory results for runoff prediction. Both models give more accurate predictions of runoff in response to heavy rainfall events. The 21/Oct/2013 (return period >1 year) and the 8/Nov/2014 events (return period nearly 1 year) have the highest R_t^2 values. Both models tend to underestimate the peak runoff and delay the time to peak runoff slightly for the event on 26/Aug/2015. This may reflect an overestimation of the detention effect in the drainage layer. Alternatively, the slight difference between the substrates used in TB7 and Yio et al. (2013) and the introduction of a filter sheet in the field test beds could result in an overestimation of substrate detention. The two models give consistent performance. During the heaviest 21/Oct/2013 event, the difference between the two models is minor. Richard's equation has better performance in the 24/May/2014 and 26/Aug/2015 events when the local field capacity is relatively low compared with the rest of the events. However, Richard's Equation has worse performance in the 6/Dec/2012 event, when the local field capacity is high. Except for the fact that the Richard's Equation requires several input parameters, there is no obvious advantage of the Reservoir Routing model over the Richard's Equation. The fact that the Reservoir Routing model relies on calibrated parameters which do not necessarily have physical meaning limits its generic application.

Fig. 4. Monitored and modelled runoff using the Reservoir Routing model and the Richard's Equation (Richard's Equation was implemented in MATLAB using SWRC B-Mualem model and constant suction head lower boundary condition).

This type of model validation (based on runoff) has been presented elsewhere. However, further independent validation is provided by the monitored moisture content data. Fig. 5(a) shows the dynamic responses of modelled and measured temporary storage in TB1 during the heaviest 21/Oct/2013 event. The modelled temporary storage curves were smoothed by performing 4 adjacent points regression. The modelled temporary storage is more dynamic compared with the measured, which may reflect the response rate of the moisture probes. However, the overall timing of the temporary storage is modelled well by both models, even though more water is predicted by the Richard's Equation to be stored in the substrate. Whilst in this case the Richard's Equation appears to overestimate the temporarily stored moisture, this is not always the case.

The temporarily stored runoff, modelled by the Reservoir Routing model, was converted to volumetric water content using Eq. 13. Fig. 5(b) compares observed versus modelled water content for all five selected storm events. Both the observed and modelled moisture data were recorded every 5 minutes, starting from the time when significant runoff was first observed to the end of the storm. The dotted lines represent ±5% deviation. The predictions of both models are consistent, but the Richard's Equation tends to overestimate the water content in most cases, while the Reservoir Routing model is more likely to underestimate the water content. Overall, the water content using both models is within ±5% error.

$$\boldsymbol{\theta_t} = \frac{\boldsymbol{h_t}}{\mathbf{80}} + \boldsymbol{\theta_{fc}} \tag{13}$$

where $\boldsymbol{\theta_t}$ is the volumetric water content at time $\boldsymbol{t}$, $\boldsymbol{h_t}$ is the modelled temporary storage by the Reservoir Routing model (mm), $\mathbf{80}$ is the depth of the substrate (mm), $\boldsymbol{\theta_{fc}}$ is the depth averaged local field capacity for each event**.**

As the Richard's equation is solved over a depth profile, validation of the vertical moisture content profile is possible. Fig. 5(c) compares the modelled and observed moisture content fluctuations at three depths for the 21/Oct/2013 event. This comparison reveals stronger vertical gradients in the modelled responses compared with the observed data. Potential reasons for this are explored within the discussion section.

Fig. 5. Validation of temporarily stored moisture. (a) depth averaged temporary storage; (b) scatter plot comparison of water content for all storm events (depth averaged); (c) comparison of vertical water content profiles.

4 Discussion

Modelling of green roof substrate detention using Richard's Equation requires several input parameters. Conventionally, these parameters are derived from natural soil based empirical equations. This section aims to investigate the sensitivity of the predictions to the parameters. The event on 21/Oct/2013 was used to undertake the sensitivity analysis and the influence of water release curve, hydraulic conductivity function and lower boundary condition were considered.

4.1 Water release curve

The modelling with Richard's Equation reported earlier was based on SWRC B (Fig. 3(a)), in which a Durner model was fitted to the data points determined by the hanging column and pressure plate extractor methods. In terms of fitting to measured SWRC data, the differences between SWRC B (Durner) and SWRC A (Van-Genuchten) are minor. The question raised here is whether this minor difference in SWRC could influence the overall modelling results. SWRC A (Fig. 3(a)) was used with the Mualem model to regenerate the runoff and vertical water content profile for the event on 21/Oct/2013.

Fig. 6(a) shows the monitored and modelled runoff using SWRC A-Mualem and SWRC B-Mualem model. Some noticeable differences are evident between the two models. More significant detention effects in the substrate were modelled by the SWRC A-Mualem model. The time to start of runoff was delayed by about an hour, and the model underestimated the peak runoff by nearly 60%. Fig. 6(b) presents the modelled vertical water content profile using the SWRC A-Mualem model. Compared with Fig. 5(a), in which the vertical water content profile was modelled using the SWRC B-Mualem model, significantly more water is modelled to be temporarily stored in the substrate.

In terms of SWRC, the two models both have good fits to the measured data and no notable difference was evident; however, significant differences were observed in the modelled runoff and vertical water content profile. This appears to be caused by the differences in SWRC derived HCF. As shown in Fig. 3(b), the HCFs associated with the two models show large differences. The SWRC A HCF gives lower values of unsaturated hydraulic conductivity than SWRC B, and as a consequence, more water is predicted to be stored in the substrate. More discussion on the influence of HCF is provided in section 4.2.

Fig. 6. Validation of runoff and temporarily stored moisture. (a) monitored and modelled runoff; (b) monitored and modelled vertical water content profiles using the SWRC A-Mualem model.

4.2 Hydraulic conductivity function

The Mualem equation is not independent of the SWRC; changing the SWRC also changes the HCF. As shown in Fig. 3(b), SWRC A and SWRC B lead to different estimates of the HCF. As a consequence, it is difficult to distinguish whether it is the minor difference in SWRC or the HCF that influences the predictions. In addition, as suggested in previous studies, the Mualem equation may not provide the best fit to the measured unsaturated hydraulic conductivity (Liu and Fassman-Beck, 2018). The investigation here aims to assess the influence of HCF on the predictions. The work reported earlier utilized SWRC B in combination with the Mualem HCF formulation. Here one additional option is considered: SWRC B-Eq. 10.

Figure 7(a) shows the modelled runoff using the SWRC B-Eq. 10 formula. Compared with the runoff modelled by the SWRC B-Mualem model, the peak runoff was reduced by about 70% compared with the monitored value. Figure 7(b) presents the modelled vertical water content profile using the Eq. 10 HCF. The maximum water content nearly doubled the quantity shown in Fig. 5(c). In terms of the runoff prediction and the vertical water content profile, the Richard's Equation is clearly very sensitive to the HCF, which indicates that a suitable HCF is needed to correctly characterise the dynamics of water content variation in the substrate. This observation may be even more relevant when deeper systems (e.g. intensive green roofs or bio-retention cells) are to be modelled. In this case, despite the fact that Eq. 10 appears to fit the preliminary laboratory data better than the two other options, SWRC B-Mualem appears to result in the most representative model prediction.

Fig. 7. Validation of runoff and temporarily stored moisture. (a) monitored and modelled runoff; (b) monitored and modelled vertical water content profiles using SWRC B-Eq. 10 model.

4.3 Lower boundary condition

Based on the conceptual model outlined in Fig. 1, the Richard's Equation was applied only when the substrate moisture content was between field capacity and saturation (i.e. to model the detention). Based on field observations that the water content does not decrease below field capacity following a storm event, the lower boundary of the Richard's Equation was set to a constant suction head. However, in some other studies, different approaches have been adopted. For example, Richard's Equation was used to model the retention and detention and the lower boundary was set to be free drainage in the studies of Liu and Fassman-Beck, (2017) and Palla et al., (2009,2012). The seepage boundary condition, in which the lower boundary is set as zero flux when the bottom boundary node is unsaturated and to zero pressure head when it is saturated, has also been applied to model green roof substrate with Richard's Equation (Brunetti et al., 2016; Hakimdavar et al., 2014). Model validation presented earlier has confirmed that the approach adopted in this study provides reasonable predictions of runoff and vertical water content profile. This section focuses on the influence of these alternative boundary conditions on the predictions. SWRC B was used for the SWRC and the Mualem model was adopted to represent the HCF. The lower boundary was set to be free drainage (Eq. 14) or seepage, and the runoff and the vertical water content profiles were regenerated for the event of 21/Oct/2013.

$$\frac{\partial h}{\partial Z} = 0 \quad (14)$$

Figure 8(a) shows the modelled runoff using free drainage boundary condition. Compared with the runoff modelled with constant head boundary condition, the free drainage boundary condition underestimated the second peak runoff by 13.9% and the peak runoff was also delayed by 5 minutes. The drain down of the runoff responded slower and lasted longer, the R_t^2 also dropped from 0.902 to 0.752. The long drain down curve was also observed in Liu and Fassman-Beck, (2017) when using a free drainage boundary condition. Figure 8(b) compares the monitored and modelled water content profile for the event. Following the storm event, the modelled water content dropped much faster than the monitored data and the modelled water content fell well below observed field capacity. Allowing the water content to drain below field capacity leads to an underestimation of water retained in the substrate. In the study of Palla et al. (2009), the same observation was made, using free drainage boundary condition with Richard's Equation, the model underestimated the water content for most of the studied storm events. However, compared with the vertical water content modelled with constant head boundary condition (Fig. 6(b)), the vertical gradient is less significant, and therefore more similar to the monitored data.

The unrealistic drain-down observed here under free drainage conditions suggests that it is more appropriate to set the lower boundary condition to a constant suction head when applying Richard's Equation to model the runoff from green roof substrates.

Fig. 8. Validation of runoff and temporarily stored moisture. (a) Monitored and modelled runoff; (b) monitored and modelled vertical water content profiles using SWRC B-Mualem model and free drainage boundary condition.

Figure 9(a) presents the modelled runoff using the seepage boundary condition. The timing of the runoff profile was wrongly estimated by the model using the seepage boundary condition. The time to start of runoff was delayed about 75 minutes and the time of peak runoff was also wrongly predicted; 16.17% less runoff was estimated by the model compared with the constant head option. The R_t^2 also dropped from 0.902 to 0.691. As the seepage boundary assumes zeros boundary flux when the bottom boundary is unsaturated, no outflow is generated until the lower boundary becomes saturated, and as a consequence, a delay in runoff was generated by the model. Figure 9(b) shows the modelled vertical water content profiles using the seepage boundary condition. More water was modelled to be stored in the substrate, which resulted in less runoff being generated. The moisture content at the bottom boundary corresponds to saturated volumetric water content. Following the storm event, the moisture content in the substrate was modelled to be kept at a high level, which is inconsistent with the observed moisture content data.

The wrongly modelled timing of the runoff profile and the very unrealistic vertical water content profiles produced using the seepage boundary condition indicate that it is inappropriate to set seepage as the boundary condition when using Richard's Equation to model the detention effects of the type of green roof used in this study.

Fig. 9. Validation of runoff and temporarily stored moisture. (a) Monitored and modelled runoff; (b) monitored and modelled vertical water content profiles using SWRC B-Mualem model and the seepage boundary condition.

5 Conclusions

Monitored moisture content data was used to investigate moisture content changes within a green roof substrate during storm events. It was found that once the substrate reaches field capacity, moisture responses at all three depths in an 80 mm green roof substrate occur simultaneously, rather than as a wetting front moving downwards. The maximum water holding capacity determined by FLL tests is consistent with field capacity measured in the field. The water release curve for HLS green roof substrate was characterised and it has been confirmed that the green roof substrate is more like a dual porosity system and therefore that the SWRC is better represented by the Durner equation.

Both the Richard's Equation and the lumped Reservoir Routing model can provide reasonable predictions of runoff profiles, and overall temporary storage dynamics. It should be noted that, whilst the Reservoir Routing model required calibration from observed rainfall-runoff performance data, the physically-based Richard's Equation only required data based on the measurable physical characteristics of the substrate (i.e. SWRC, HCF and field capacity). Validated by five storm events, the approach of using Richard's Equation to represent temporary (detention) moisture storage between field capacity and saturation proposed in this paper was proved to be capable of regenerating observed runoff profiles.

Discrepancies between the measured and modelled (Richard's Equation) vertical depth profiles indicate further research is required to investigate the green roof substrate's unsaturated hydraulic conductivity. Sensitivity analysis conducted with the Richard's Equation suggested that the modelled runoff profile and vertical water content profile is sensitive to the HCF.

The lower boundary condition has a significant impact on predictions of both runoff and vertical water content profile in the substrate. It is concluded that neither free drainage nor seepage boundary conditions are suitable boundary conditions to use with Richard's Equation to model the detention effects of the green roof used in this study. However the constant suction head boundary condition was found to represent the observed behaviour better.

6 Acknowledgements

Zhangjie Peng is supported by the University of Sheffield, Faculty of Engineering Doctoral Academy Award. The authors would like to thank Dr. Simon De-Ville, Dr. Christian Berretta and Dr. Simon Poë for their contribution in establishing the monitoring programme.

7 References

ASTM, 2015. Standard Test Methods for measurement of hyraulic conductivity of unsaturated soils, Astm. https://doi.org/10.1520/D7664

Berretta, C., Poë, S., Stovin, V., 2014. Moisture content behaviour in extensive green roofs during dry periods: The influence of vegetation and substrate characteristics. J. Hydrol. 511, 374–386. https://doi.org/10.1016/J.JHYDROL.2014.01.036

Brunetti, G., Šimůnek, J., Piro, P., 2016. A Comprehensive Analysis of the Variably Saturated Hydraulic Behavior of a Green Roof in a Mediterranean Climate. Vadose Zo. J. 15, 0. https://doi.org/10.2136/vzj2016.04.0032

Castiglia Feitosa, R., Wilkinson, S., 2016. Modelling green roof stormwater response for different soil depths. Landsc. Urban Plan. 153, 170–179. https://doi.org/10.1016/J.LANDURBPLAN.2016.05.007

De-Ville, S., Menon, M., Jia, X., Reed, G., Stovin, V., 2017. The impact of green roof ageing on substrate characteristics and hydrological performance. J. Hydrol. 547, 332–344. https://doi.org/10.1016/j.jhydrol.2017.02.006

De-Ville, S., Menon, M., Stovin, V., 2018. Temporal variations in the potential hydrological performance of extensive green roof systems. J. Hydrol. 558, 564–578. https://doi.org/10.1016/j.jhydrol.2018.01.055

Durner, W., 1994. Hydraulic conductivity estimation for soils with heterogeneous pore structure. Water Resour. Res. 30, 211–223. https://doi.org/10.1029/93WR02676

Fassman, E., Simcock, R., 2012. Moisture Measurements as Performance Criteria for Extensive Living Roof Substrates. J. Environ. Eng. 138, 841–851. https://doi.org/10.1061/(ASCE)EE.1943-7870.0000532

FLL, 2008. FLL (Forschungsgesellschaft Landschaftsentwicklung Landschaftsbau), (2008). Guidelines for the Planning, Construction and Maintenance of Green Roofing.

Forschungsgesellschaft Landschaftsentwicklung Landschaftsbau e. V., Bonn, Germany. 119.

Hakimdavar, R., Culligan, P.J., Finazzi, M., Barontini, S., Ranzi, R., 2014. Scale dynamics of extensive green roofs: Quantifying the effect of drainage area and rainfall characteristics on observed and modeled green roof hydrologic performance. Ecol. Eng. 73, 494–508. https://doi.org/10.1016/J.ECOLENG.2014.09.080

Hilten, R.N., Lawrence, T.M., Tollner, E.W., 2008. Modeling stormwater runoff from green roofs with HYDRUS-1D. J. Hydrol. 358, 288–293. https://doi.org/10.1016/j.jhydrol.2008.06.010

Kasmin, H., Stovin, V.R., Hathway, E.A., 2010. Towards a generic rainfall-runoff model for green roofs. Water Sci. Technol. 62, 898. https://doi.org/10.2166/wst.2010.352

Liu, R., Fassman-Beck, E., 2018. Pore Structure and Unsaturated Hydraulic Conductivity of Engineered Media for Living Roofs and Bioretention Based on Water Retention Data. J. Hydrol. Eng. https://doi.org/10.1061/(ASCE)HE.1943-5584.0001621.

Liu, R., Fassman-Beck, E., 2018. Pore Structure and Unsaturated Hydraulic Conductivity of Engineered Media for Living Roofs and Bioretention Based on Water Retention Data. J. Hydrol. Eng. https://doi.org/10.1061/(ASCE)HE.1943-5584.0001621

Liu, R., Fassman-Beck, E., 2017. Hydrologic response of engineered media in living roofs and bioretention to large rainfalls: experiments and modeling. Hydrol. Process. 31, 556–572. https://doi.org/10.1002/hyp.11044

Liu, R., Fassman-Beck, E., 2016. Effect of Composition on Basic Properties of Engineered Media for Living Roofs and Bioretention. J. Hydrol. Eng. 21, 06016002.

https://doi.org/10.1061/(ASCE)HE.1943-5584.0001373.

Marshall, T.J., Holmes, J.W., Rose, C.W., 1996. Soil Physics. Cambridge University Press. https://doi.org/10.1017/CBO9781139170673

Mualem, Y., 1976. A new model for predicting the hydraulic conductivity of unsaturated porous media. Water Resour. Res. 12, 513–522. https://doi.org/10.1029/WR012i003p00513

Palla, A., Gnecco, I., Lanza, L.G., 2012. Compared performance of a conceptual and a mechanistic hydrologic models of a green roof. Hydrol. Process. 26, 73–84. https://doi.org/10.1002/hyp.8112

Palla, A., Gnecco, I., Lanza, L.G., 2009. Unsaturated 2D modelling of subsurface water flow in the coarse-grained porous matrix of a green roof. J. Hydrol. 379, 193–204. https://doi.org/10.1016/j.jhydrol.2009.10.008

Peng, Z., Stovin, V., 2017. Independent Validation of the SWMM Green Roof Module. J. Hydrol. Eng. 22, 1–12. https://doi.org/10.1061/(ASCE)HE.1943-5584.0001558.

Poë, S., Stovin, V., Berretta, C., 2015. Parameters influencing the regeneration of a green roof's retention capacity via evapotranspiration. J. Hydrol. 523, 356–367. https://doi.org/10.1016/J.JHYDROL.2015.02.002

Seki, K., 2010. SWRC fit: a nonlinear fitting program with a water retention curve for soils having unimodal and bimodal pore structure. Hydrol. Earth Syst. Sci. Discuss. 4, 407–437. https://doi.org/10.5194/hessd-4-407-2007

Soulis, K.X., Valiantzas, J.D., Ntoulas, N., Kargas, G., Nektarios, P.A., 2017. Simulation of green roof runoff under different substrate depths and vegetation covers by coupling a simple conceptual and a physically based hydrological model. J. Environ. Manage. 200, 434–445. https://doi.org/10.1016/j.jenvman.2017.06.012

Stovin, V., Poë, S., De-Ville, S., Berretta, C., 2015. The influence of substrate and vegetation configuration on green roof hydrological performance. Ecol. Eng. 85, 159–172. https://doi.org/10.1016/j.ecoleng.2015.09.076

Stovin, V., Vesuviano, G., De-Ville, S., 2017. Defining green roof detention performance. Urban Water J. 14, 574–588. https://doi.org/10.1080/1573062X.2015.1049279

Stovin, V., Vesuviano, G., Kasmin, H., 2012. The hydrological performance of a green roof test bed under UK climatic conditions. J. Hydrol. 414–415, 148–161. https://doi.org/10.1016/J.JHYDROL.2011.10.022

van Genuchten, M.T., 1980. A Closed-form Equation for Predicting the Hydraulic Conductivity of Unsaturated Soils1. Soil Sci. Soc. Am. J. 44, 892. https://doi.org/10.2136/sssaj1980.03615995004400050002x

Vesuviano, G., Sonnenwald, F., Stovin, V., 2014. A two-stage storage routing model for green roof runoff detention. Water Sci. Technol. 69, 1191. https://doi.org/10.2166/wst.2013.808

Vesuviano, G., Stovin, V., 2013. A generic hydrological model for a green roof drainage layer. Water Sci. Technol. 68, 769. https://doi.org/10.2166/wst.2013.294

Voyde, E., Fassman, E., Simcock, R., Wells, J., 2010. Quantifying Evapotranspiration Rates for New Zealand Green Roofs. J. Hydrol. Eng. 15, 395–403. https://doi.org/10.1061/(ASCE)HE.1943-5584.0000141

Yio, M.H.N., Stovin, V., Werdin, J., Vesuviano, G., 2013. Experimental analysis of green roof substrate detention characteristics. Water Sci. Technol. 68, 1477–1486. https://doi.org/10.2166/wst.2013.381

Young, P., Jakeman, A., McMurtrie, R., 1980. An instrumental variable method for model order identification. Automatica 16, 281–294. https://doi.org/10.1016/0005-1098(80)90037-0

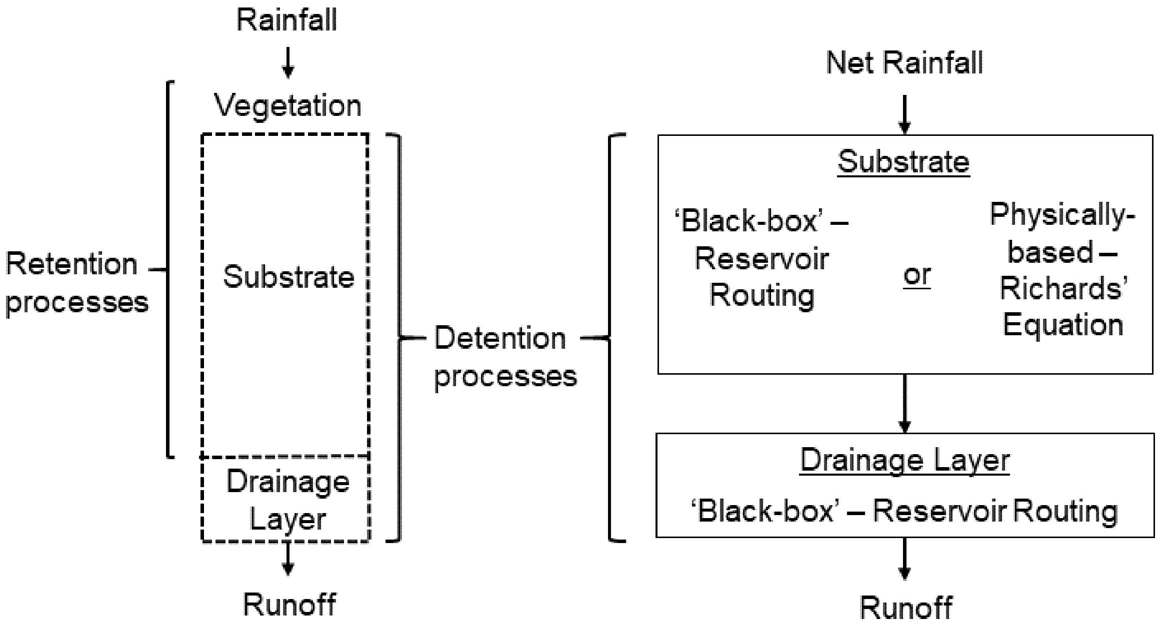

Fig. 1. Conceptual green roof hydrological model: left – vertical profile through a typical green roof system indicating the layers associated with retention and detention processes; right – components of a two-stage detention model, indicating the two alternative options for representing substrate detention considered in the present paper.

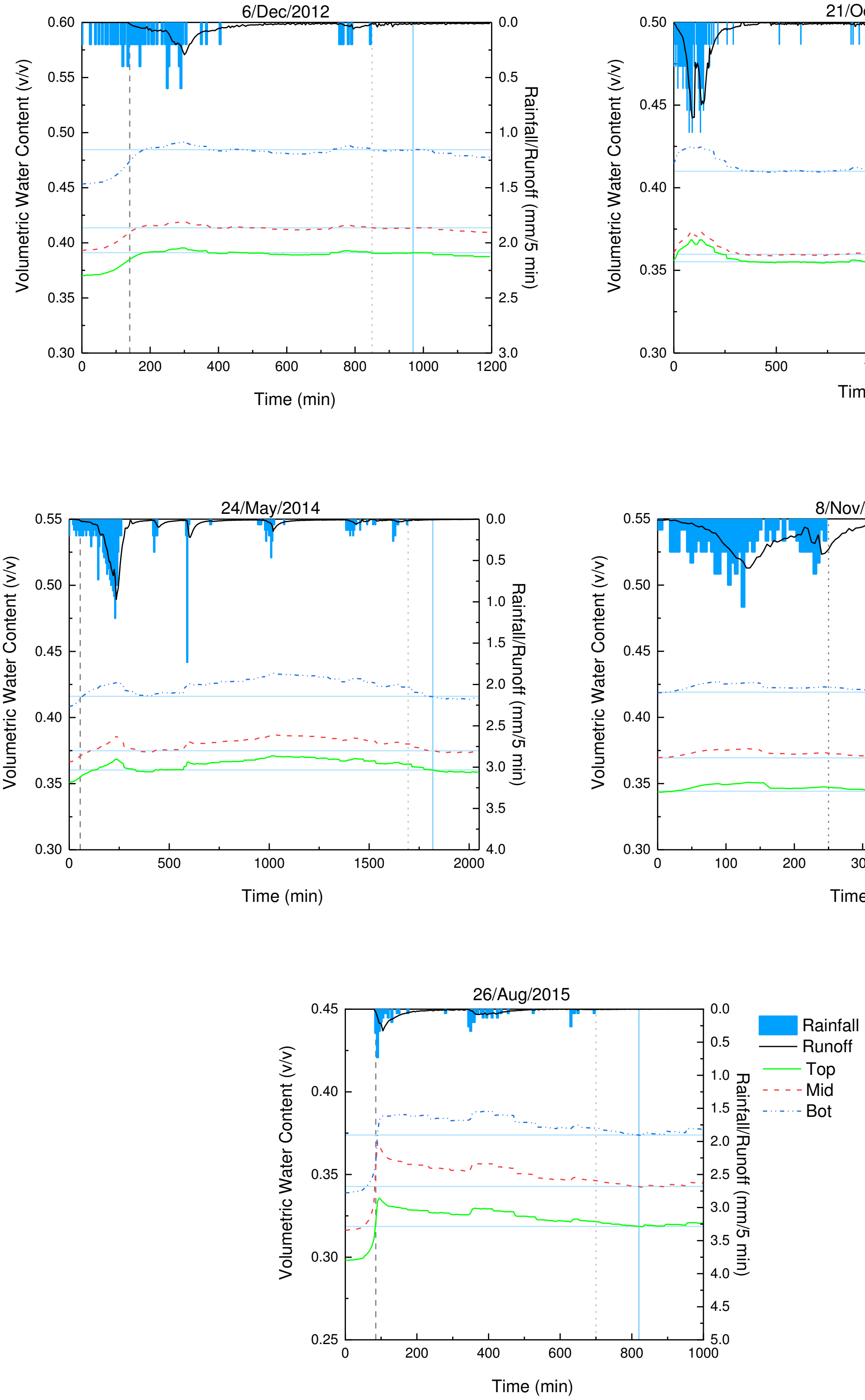

Fig. 2. Monitored rainfall, runoff and moisture content profiles for the five selected storm events (vertical dashed line indicates the time significant runoff was firstly observed, dotted line represents the time rainfall stops, the solid vertical line is the time two hours after rainfall stops and the corresponding volumetric water content is assumed to indicate local field capacity).

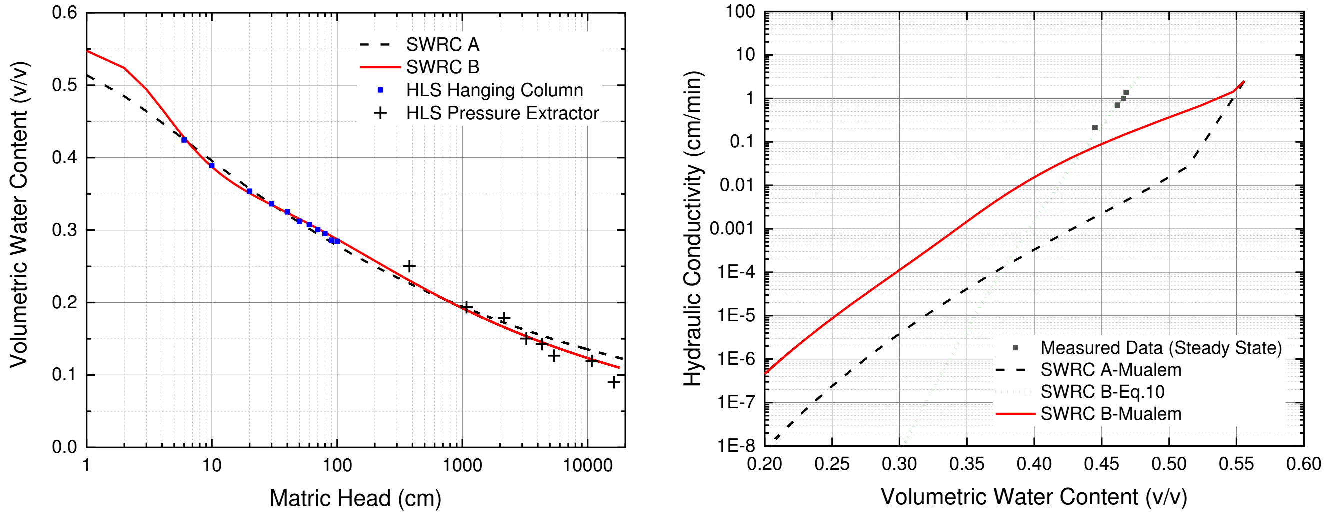

(a) (b)

Fig. 3. Water release curves and hydraulic conductivity functions. (a) SWRC A is fitted by the Van-Genuchten model, SWRC B is fitted by the Durner model, both models were fitted using hanging column and pressure plate extractor data; (b) plots of the new HCF and the HCFs derived from the two SWRC in (a) via the Mualem model.

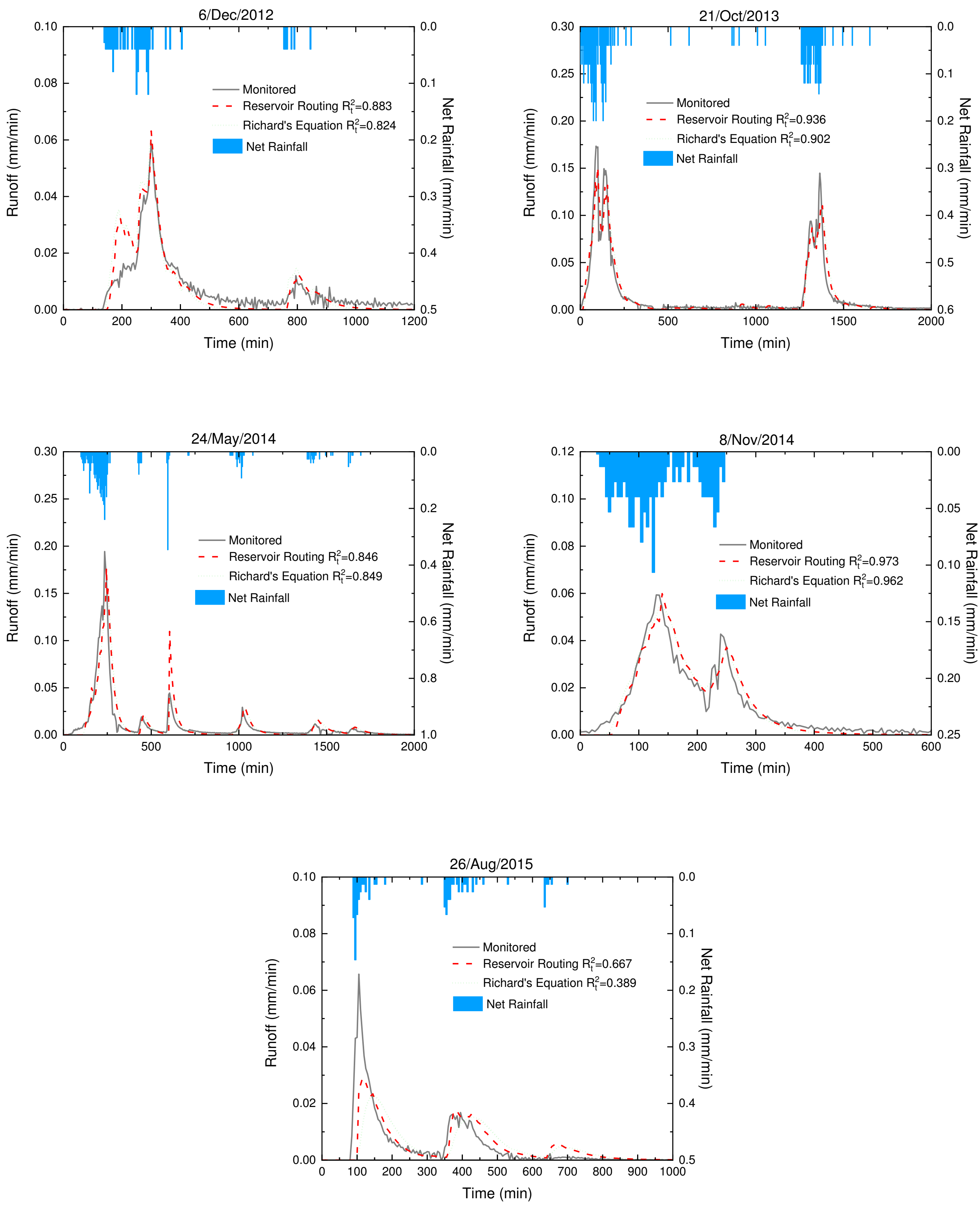

Fig. 4. Monitored and modelled runoff using the Reservoir Routing model and the Richard's Equation (Richard's Equation was implemented in MATLAB using SWRC B-Mualem model and constant suction head boundary condition).

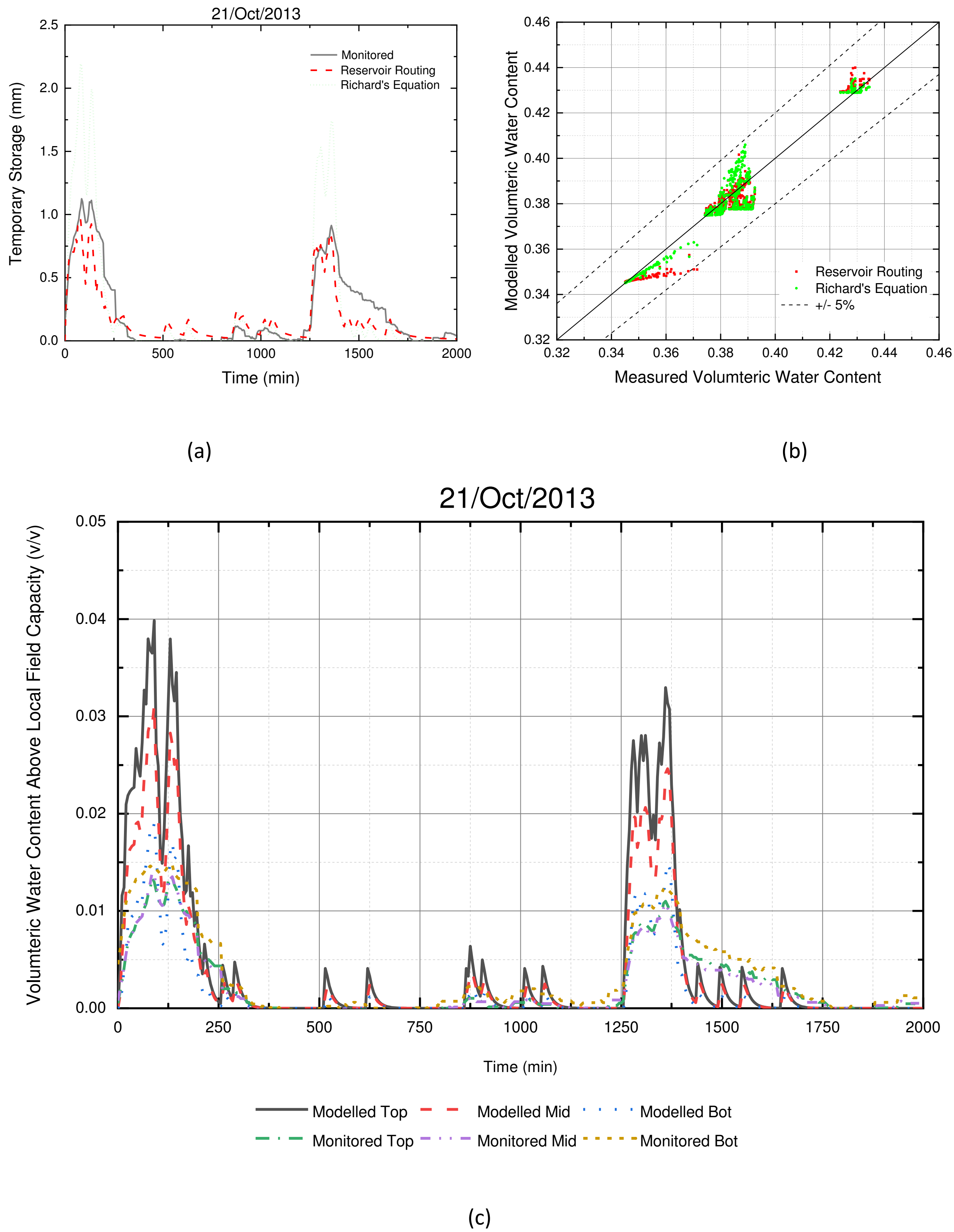

Fig. 5. Validation of temporarily stored moisture. (a) depth averaged temporary storage; (b) scatter plot comparison of water content for all storm events (depth averaged); (c) comparison of vertical water content profiles.

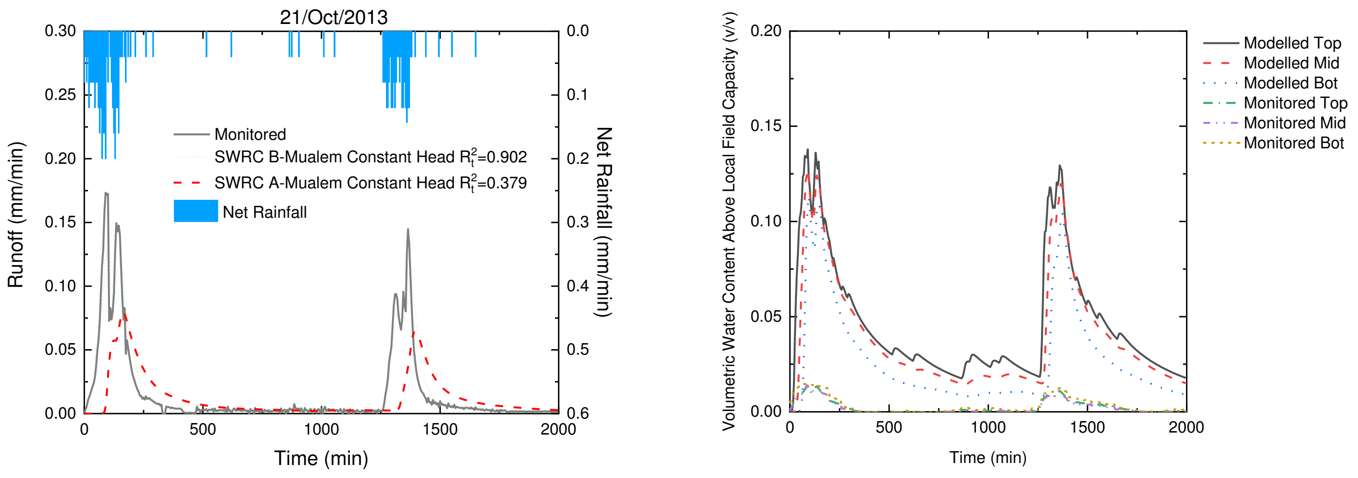

(a) (b)

Fig. 6. Validation of runoff and temporarily stored moisture. (a) monitored and modelled runoff; (b) monitored and modelled vertical water content profiles using the SWRC A-Mualem model.

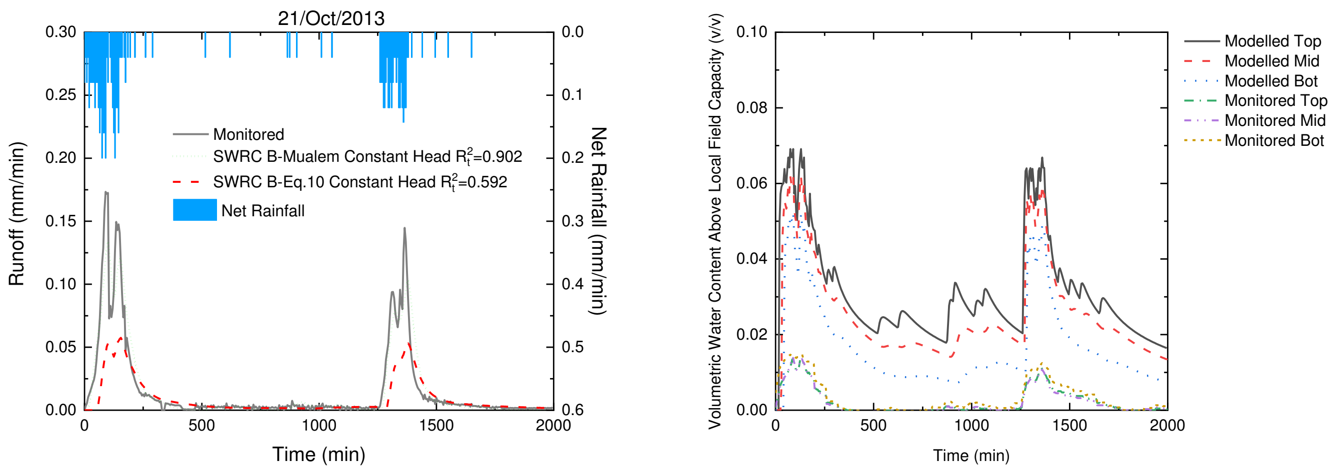

(a) (b)

Fig. 7. Validation of runoff and temporarily stored moisture. (a) monitored and modelled runoff; (b) monitored and modelled vertical water content profiles using SWRC B-Eq. 10 model.

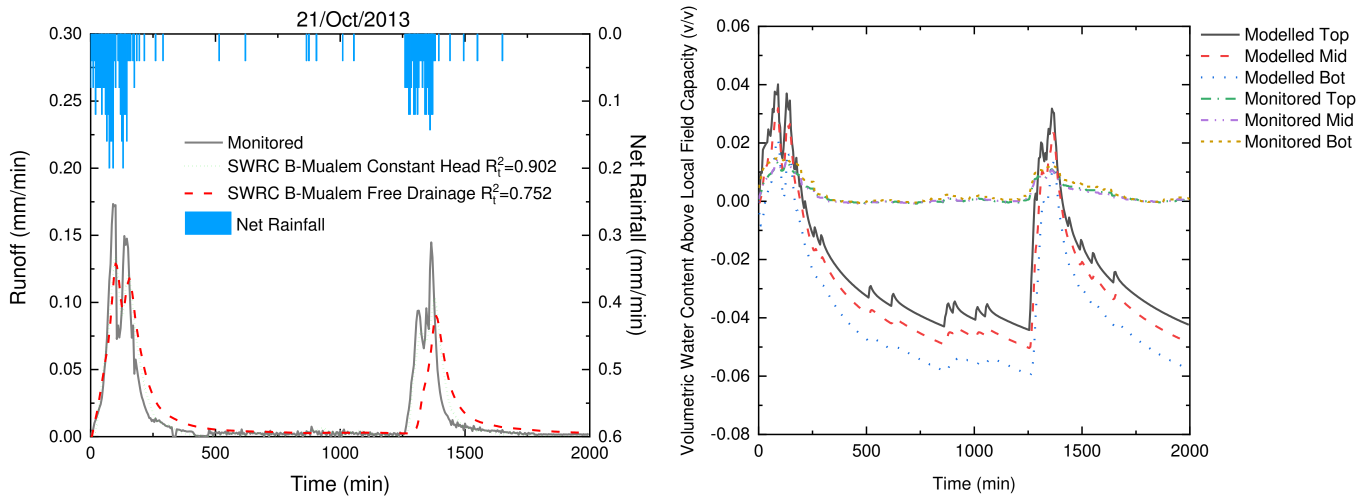

(a) (b)

Fig.8. Validation of runoff and temporarily stored moisture. (a) Monitored and modelled runoff; (b) monitored and modelled vertical water content profiles using SWRC B-Mualem model and free drainage boundary condition.

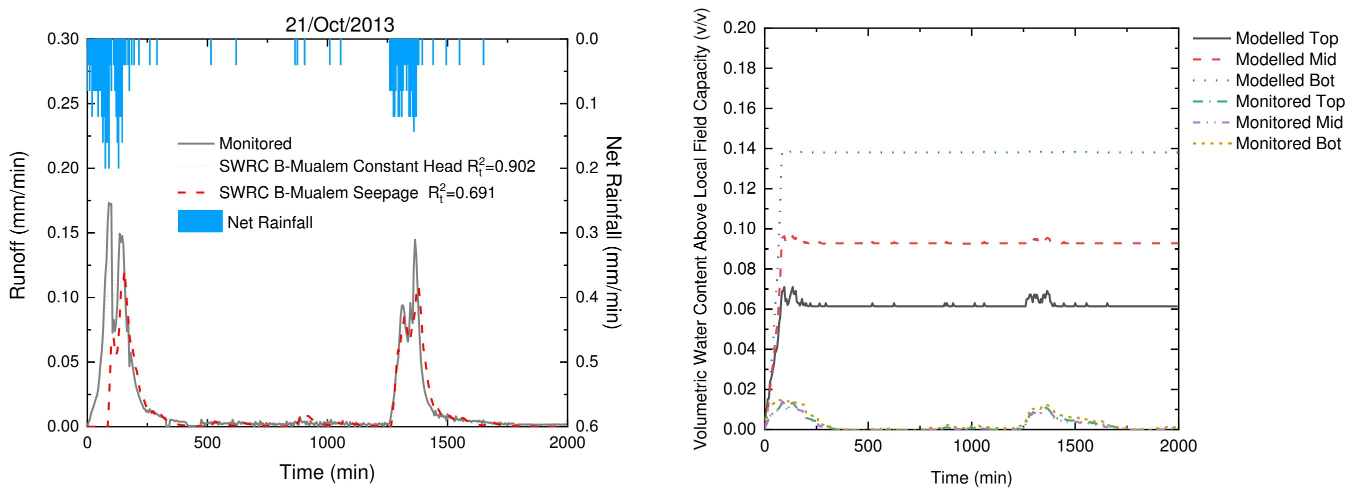

(a) (b)

Fig. 9. Validation of runoff and temporarily stored moisture. (a) Monitored and modelled runoff; (b) monitored and modelled vertical water content profiles using SWRC B-Mualem model and the seepage boundary condition.

Table 1. Value of parameters used in the Reservoir Routing model

Parameter	Value	
	TB7	TB1
k_g	0.212	0.175
n_g	2.000	2.000
k_D	0.026	0.026
n_D	1.196	1.196

Table 2. Hydrological characteristics of the five selected storm events and TB1 hydrological performance

Event No.	Date	Rainfall Duration (h)	Rainfall depth (mm)	ADWP (h)	Peak rainfall intensity (mm/5 min)	Return Period (yr)	Retention (%)	Initial water content			
								Top	Mid	Bot	Mean
228	06/Dec/2012	14.02	12.20	70.43	0.60	<1	29.97	0.37	0.393	0.453	0.406
292	21/Oct/2013	27.35	31.80	10.90	1.00	>1	0	0.356	0.36	0.414	0.377
361	24/May/2014	28.22	24.13	16.63	1.73	<1	8.73	0.351	0.366	0.408	0.375
396	08/Nov/2014	4.43	8.40	15.52	0.36	<1	6.21	0.344	0.37	0.419	0.377
458	26/Aug/2015	11.63	13.00	57.23	2.67	<1	60.81	0.298	0.316	0.339	0.318

Table 3. Local field capacity determined for each storm event

Event No.	Date	Local field capacity TB1			
		Top	Mid	Bot	Mean
228	06/Dec/2012	0.391	0.414	0.485	0.430
292	21/Oct/2013	0.355	0.360	0.410	0.375
361	24/May/2014	0.360	0.375	0.416	0.384
396	08/Nov/2014	0.344	0.396	0.419	0.387
458	26/Aug/2015	0.319	0.343	0.374	0.345
Overall mean					0.384

Table 4. HLS Substrate characteristics according to FLL (2008) test methods

Properties	Unit	Mean	St.Dev
Particle size <0.063 mm	%	2.72	0.25
d_{50}	mm	5.05	0.07
Bulk density	g/cm^3	0.81	0.05
Porosity	%	58.10	0.85
Maximum water holding capacity	%	38.53	0.60
Permeability	mm/min	25	7.16

Table 5. Fitted parameters for the water release curves for the HLS substrate

Van-Genuchten (SWRC A)		Durner (SWRC B)	
Parameter	Value	Parameter	Value
Θ_s	0.556	Θ_s	0.556
Θ_r	0	Θ_r	0
α	0.807	α_1	0.306
n	1.157	n_1	2.255
		α_2	0.02
		n_2	1.194
		w_1	0.378
R^2	0.995	R^2	0.988